NEOPLASIA
www.neoplasia.com

Volume 22 Number 9 September 2020 pp. 365–375

Dual inhibition of VEGF and PARP suppresses KRAS-mutant colorectal cancer

Longhui Zhong [a,1]; Rong Wang [a,1]; Yanxia Wang [a]; Shunli Peng [a]; Yueyun Ma [a]; Sijie Ding [a]; Hong Yang [a,b]; Shiyu Chen [a]; Xiaoqing Luo [a]; Wei Wang [a,*]

[a] Department of Radiation Oncology, Nanfang Hospital, Southern Medical University, Guangzhou 510515, PR China; [b] Department of Oncology, Hunan Provincial People's Hospital and The First Affiliated Hospital of Hunan Normal University, Changsha 410002, Hunan, PR China

Abstract

The addition of bevacizumab to chemotherapy has prolonged overall and progression-free survival rates for metastatic colorectal cancer (mCRC). However, KRAS-mutant (KRAS-mut) CRC, lacking an ideal targeted agent, represents an inferior-response subgroup of patients. In the present study, we investigated a combination approach of bevacizumab + olaparib in KRAS-mut CRC in a preclinical setting. The combined therapy effectively prevented tumor growth in a KRAS-mut cancer cell-derived xenograft model, although this effect was not observed *in vitro*. Under bevacizumab treatment, we detected intratumor hypoxia and impaired homologous recombination repair (HRR), accompanied by vascular regression. We explored the underlying mechanism of this combined therapy by mimicking a hypoxic condition *in vitro* using cobalt chloride ($CoCl_2$). The results showed that hypoxia impairs HRR and therefore sensitized KRAS-mut CRC cell lines HCT-116, SW620, and Lovo to olaparib. Furthermore, under this hypoxic condition, olaparib could arrest the cell cycle in the G2/M phase, increase DNA damage and dramatically induce cell apoptosis in KRAS-mut CRC cells. Taken together, these results indicated that the combination of bevacizumab + olaparib could be a potential therapeutic approach in a KRAS-mut CRC cohort.

Neoplasia (2020) 22 365–375

Keywords: Olaparib, Bevacizumab, Homologous-recombination repair, KRAS, Colorectal cancer

Introduction

Colon or rectal (colorectal) cancer (CRC) is the third-leading cause of cancer-related mortality [1]. At the time of diagnosis, 30% of CRC patients present metastases [2], and there is an even higher metastasis rate of 55.9% in KRAS-mutant (KRAS-mut) CRC patients [3]. Metastatic CRC (mCRC) patients with KRAS have poorer progression-free survival (PFS) and overall survival (OS) rates than patients without KRAS mutations [4]. In addition, KRAS mutation is associated with resistance to anti–epidermal growth factor receptor (EGFR) therapy [5–9] and increases the risk of recurrence and death in CRC [10,11].

KRAS mutations are frequently detected in pan-cancers, including 97.7% of pancreatic ductal adenocarcinomas, 30.9% of lung adenocarcinomas, and approximately 44.7% of colorectal adenocarcinomas [12]. Ras mutations render Ras persistently guanosine-5′-triphosphate (GTP)-bound and constitutively active, and thus permanent Ras signaling is activated [13]. However, due to the picomolar binding affinity of small GTPases for GTP, millimolar GTP cellular concentrations, and lack of amenable deep pockets in Ras, high-affinity small-molecule antagonists have not been feasible [14,15]. Some attempts to target Ras downstream effectors—e.g., the rapidly accelerated fibrosarcoma (RAF)/mitogen-activated protein kinase kinase (MEK)/extracellular signal-regulated kinase (ERK) and phosphatidylinositol-4,5-bisphosphate 3-kinase (PI3K)/protein kinase B (Akt)/mammalian target of rapamycin (mTOR) signaling pathways [16,17]—have been unsuccessful due to poor efficacy in KRAS-mut cancers [18–21]. KRAS-mut malignancies therefore remain

Abbreviations: mCRC, metastatic colorectal cancer, HR, homologous recombination, HRR, homologous-recombination repair, $CoCl_2$, cobalt chloride, CRC, colorectal cancer, PFS, progression-free survival, OS, overall survival, EGFR, epidermal growth factor receptor, VEGF-A, vascular endothelial growth factor A, PARP, poly (adenosine diphosphate [ADP]-ribose) polymerase, SSB, single-strand break, DSB, double-strand break, BER, base excision repair

* Corresponding author.
e-mail address: wangwei9500@hotmail.com (W. Wang).

[1] These authors contributed equally to this work.

https://doi.org/10.1016/j.neo.2020.06.001

refractory, and no therapeutic agent directly targeting Ras has been approved for clinical use so far.

Bevacizumab, as a humanized monoclonal antibody that inhibits vascular endothelial growth factor A (VEGF-A), has been approved for the treatment of patients with mCRC [22]. In both first- and second-line settings, bevacizumab in combination with cytotoxic chemotherapy dramatically improved OS and PFS rates of mCRC patients [23–26]. However, although it significantly inhibits tumor growth by preventing formation of new blood vessels, bevacizumab might lose its therapeutic effect due to drug resistance [27–29]. Intratumor hypoxia induced by anti-angiogenic treatment could be an important resistant mechanism to bevacizumab that further enhances tumor growth and invasion [30–33]. On the other hand, it is well attested that hypoxia suppresses HR by downregulating HR repair (HRR) proteins, such as *BRCA1* and *RAD51*, hence increases sensitivity to PARP inhibition [34–36]. Therefore, we hypothesized that bevacizumab induced-tumor hypoxia might increase sensitivity to PARP inhibitor, thus overcome bevacizumab resistance.

Bevacizumab + olaparib has been clinically confirmed as efficacious and safe in advanced solid tumors [37]. A recent phase 3 trial confirmed that the addition of maintenance olaparib to bevacizumab provided significant PFS benefit in patients with advanced ovarian cancer, regardless of breast cancer gene (*BRCA*) mutation status [38]. Olaparib is one of the typical poly (adenosine diphosphate [ADP]–ribose) polymerase (PARP) inhibitors that have been approved in advanced epithelial ovarian or metastatic breast cancer patients with deleterious or suspected deleterious germline or somatic *BRCA* mutations (*gBRCAm* or *sBRCAm*, respectively) [39]. PARP repairs DNA single-strand breaks (SSBs) through the base excision repair (BER) pathway [40]; PARP inhibitors compromise this pathway by blocking PARP enzymatic activity, resulting in the conversion of SSBs to double-strand breaks (DSBs) during DNA replication. Normally, DSBs are repaired via the homologous-recombination (HR) pathway, which involves proteins such as *BRCA1*, *BRCA2*, and *RAD51* [40]. However, whether such a combination could be applied in KRAS-mut CRC, and the underlying mechanism by which it would work, remain unclear.

Based on all of the above, we proposed that a PARP inhibitor combined with an anti-angiogenic agent might have a synergistic effect in KRAS-mut CRC. Our results confirmed that bevacizumab treatment induced vascular regression and intratumor hypoxia, which led to HR deficiency and thus sensitized cancer cells to the PARP inhibitor olaparib.

Materials and methods

Cell cultures and reagents

We purchased 5 human KRAS-mut cell lines (HCT116, SW620, Lovo, HT29, and SW480) from the American Type Culture Collection (ATCC; Manassas, Virginia, US). Tumor cell culture was maintained in Roswell Park Memorial Institute (RPMI)-1640 medium supplemented with 10% fetal bovine serum (FBS), penicillin (100 U/mL), and streptomycin (50 mg/mL) in a humidified CO_2 incubator at 37 °C. All of the cells were passaged for <3 months before renewal from frozen, early-passage stocks. We obtained olaparib and bevacizumab from Selleck Chemicals (Houston, Texas, US) and cobalt chloride ($CoCl_2$) from Sigma-Aldrich (Saint Louis, Missouri, US). Olaparib was dissolved in dimethyl sulfoxide (DMSO) to a final concentration of 50 mmol/L; $CoCl_2$ was dissolved in double-distilled water to a concentration of 100 mmol/L and stock. Both were then stored at −20 °C.

Cell viability assay

Using the 3-(4,5-dimethylthiazol-2yl)-2,5-diphenyltetrazolium bromide (MTT) dye reduction method [41], we measured cell proliferation. Briefly, tumor cells were plated at a density of 2×10^3 cells in 100 μL RPMI-1640 plus 10% FBS per well in 96-well plates and incubated for 24 h. Next, we added bevacizumab, olaparib, or $CoCl_2$ to each well and continued incubation for another 72 h. Then, 50 μL stock MTT solution (2 mg/ml; Sigma-Aldrich) was added to all wells, and the cells were incubated for 2 h at 37 °C. We then removed the media containing the MTT solution and dissolved the dark-blue crystals by adding 100 μL DMSO. Absorbance was measured with an MTP-120 microplate reader (Corona Electric, Corona, New York, US) at test and reference wavelengths of 490 and 550 nm, respectively.

Antibodies and Western blot analysis

We separated protein aliquots (20 μg) on sodium dodecyl sulfate polyacrylamide gel electrophoresis (SDS-PAGE) gel (Bio-Rad, Hercules, California, US) and transferred them to polyvinylidene difluoride (PVDF) membranes (Bio-Rad). The membranes were washed 3 times and incubated with blocking solution for 1 h at room temperature (RT). After washing, we incubated the membranes overnight at 4 °C with primary antibodies against Poly (ADP-Ribose) Polymer (PAR) antibody (ab14460; Abcam, Cambridge, UK), hypoxia-inducible factor 1 alpha (HIF-1α; 20960-1-AP; Proteintech, Wuhan, China), and β-actin (Cell Signaling Technology [CST], Danvers, Massachusetts, US). Next, we washed and incubated the membranes for 1 h at RT with species-specific horseradish peroxide (HRP)-conjugated secondary antibodies. Finally, using an enhanced-chemiluminescent (ECL) substrate (Thermo Fisher Scientific, Waltham, Massachusetts, US), we visualized immunoreactive bands. All of the data are representative of 3 independent experiments.

Reverse-transcription and quantitative real-time PCR (qRT-PCR)

We isolated total ribonucleic acid (RNA) from cells or tumor tissues using RNAiso Plus (TaKaRa, Dalian, China) and reverse-transcribed it into complementary DNA (cDNA) using PrimeScript RT Master Mix (TaKaRa) per manufacturer's instructions. Quantitative real-time PCR (qRT-PCR) was performed using a Roche LightCycler 480 system (Roche Diagnostics, Meylan, France) with SYBR Premix Ex Taq (Tli RNase H Plus; TaKaRa). Oligonucleotide primers used for *RAD51* and glyceraldehyde 3-phosphate dehydrogenase (GAPDH; internal control) were as follows: *RAD51*: 5′-CAACCCATTTCACGGTTAGAGC-3′ (sense); 5′-TTCTTTGGCGATAGGCAACA −3′ (antisense); GAPDH: 5′-AGAA GGTGGGGCTCATTTG-3′ (sense); 5′-AGGGGCCATCCACAGTC TTC-3′ (antisense). All reactions were performed in triplicate for each sample. Cycle threshold (Ct) values of *RAD51* cDNA were normalized to GAPDH using the $-2^{\Delta\Delta Ct}$ method.

Apoptosis and cell cycle analyses

We seeded cells at a density of 2×10^5 cells/well into 6-well plates in RPMI-1640 medium with 10% FBS. After incubation for 24 h, we added various reagents to each well and continued incubation for another 72 h, after which we harvested cells and washed them once with phosphate-buffered saline (PBS). Apoptosis was measured with an Annexin V-Fluorescein Isothiocyanate (FITC)/Propidium Iodide (PI) Cell Apoptosis Detection Kit (TransGen Biotech Co., Ltd., Beijing, China) per manufacturer's protocols. Cell cycle arrest was measured with a Cell Cycle Staining Kit (Hangzhou Multi-Sciences Biotech Co., Ltd., Hangzhou, China) per manufacturer's protocols. We performed both analyses using a FACSCalibur using CellQuest software (BD FACS Aria; BD Biosciences, Franklin Lakes, New Jersey, US). All of the experiments were performed at least 3 times.

Subcutaneous xenografts in BALB/c-nu/nu nude mice

We injected suspensions of 5×10^6 HCT116 cells subcutaneously into the right hind limbs of 5- to 7-week-old female BALB/c-nu/nu nude mice, which we purchased from the Experimental Animal Center of Southern Medical University (Guangzhou, China; $N = 24$). When tumor volume reached approximately 150 mm^3, calculated as:

$$mm^3 = width^2 \times length/2,$$

we randomized the mice into 4 groups that received oral olaparib (50 mg/kg/d; $n = 6$), intraperitoneal bevacizumab (5 mg/kg/twice weekly; $n = 6$), olaparib + bevacizumab ($n = 6$), or vehicle control ($n = 6$). Tumor volume and mouse body weights were measured twice weekly. All of the animal experiments were carried out in strict accordance with the principles and procedures approved by the Committee on the Ethics of Animal Experiments of Southern Medical University (Guangzhou, China).

Immunohistochemistry (IHC)

We performed IHC staining on tissues (5 mm thick) harvested from the xenografts. Tissue sections were fixed overnight in 4% formaldehyde and then embedded in paraffin for IHC. After deparaffinization and hydration, we pretreated the sections for 20 min with 10 mmol/L sodium citrate buffer in a microwave for antigen retrieval. Next, the tissue sections were incubated overnight at 4 °C with antibodies against Ki-67 (CST), Cluster of Differentiation 31 (CD31; Abcam), and HIF-1α (Proteintech). After incubation with a secondary antibody and treatment with the Histofine Simple Stain MAX-PO Kit (Nichirei, Tokyo, Japan), we visualized peroxidase activity via a 3,3′-Diaminobenzidine (DAB) reaction. The sections were counterstained with hematoxylin. Finally, all of the sections were stained with hematoxylin and eosin (H&E) for routine histological examinations.

Quantification of IHC results

For Ki-67 and CD31 IHC staining, we selected the 5 areas per section showing the highest levels of staining intensity for histological quantification by light microscopy at 200 × magnification. The IHC score of HIF-1α was the product of the staining intensity and the percentage of positive cells. Staining intensity was graded on a scale of 0 to 3+ (0 for colorless, 1+ for pale yellow, 2+ for brown–yellow, and 3+ for saddle brown). Percentage of positive cells was scored on a scale of 0 to 4+ (0 for negative, 1+ for <10% positive cells, 2+ for 10–50% positive cells, 3+ for 51–75% positive cells, and 4+ for >75% positive cells). All of the results were independently evaluated by 2 authors (Longhui Zhong and Rong Wang).

Immunofluorescence staining

HCT116, Lovo and SW620 cells were plated overnight in chambered slides (1×10^4 cells/chamber) (Idibi, Germany). Cells were treated with or without $CoCl_2$ (100 μM) and/or olaparib (30 μM) for 24 h. Cells were washed with PBS and fixed in 4% paraformaldehyde at room temperature for 20 min. Then, Cells were permeabilized (0.3% Triton X-100 in PBS, 10 min) and blocked in 10% goat serum at room temperature for 1 h. Cells were incubated overnight at 4 °C with primary antibody for RAD51 (1:200 dilution) (Proteintech, Wuhan, China) or γ-H2AX - Ser139 (1:200 dilution) (CST, Danvers, MA). After three times washing with PBS, cells were incubated with Alexa Fluor 488-labeled goat antirabbit IgG (H + L) antibody (1:500 dilution) for 1 h at RT. Nuclear was stained with DAPI (Beyotime, Shanghai, China) for 5 min at RT.

For tumor tissue, tissue sections were fixed overnight in 4% formaldehyde and then embedded in paraffin. After deparaffinization and hydration of 4-μm-sliced sections, heat-induced antigen retrieval was performed. The primary antibody (anti-RAD51) was applied and incubated overnight at 4 °C. After Alexa Fluor 488-labeled goat antirabbit IgG (H + L) antibody (1:500 dilution) (Beyotime, Shanghai, China) was applied, slides were stained with DAPI (Beyotime, Shanghai, China) for 5 min.

Images from random fields were acquired with an OLYMPUS BX63 fluorescence microscope (OLYMPUS, Tokyo, Japan). For quantification of RAD51 foci and γ-H2AX foci, at least 100 cells from each group were visually scored. Cells showing more than 3 foci were counted as positive for γ-H2AX or RAD51.

Statistical analysis

Data from the tumor progression of xenografts are expressed as means þ standard error (SE), and data from other experiments are expressed as means þ standard deviation (SD). Comparisons between 2 groups were analyzed using Student's t test, those between >2 groups using 1-way analysis of variance (ANOVA). $P < 0.05$ (2-sided) was considered statistically significant. All of the statistical analyses were performed using SPSS software version 20 (IBM Corp., Armonk, New York, US).

Results

No combination benefit was observed in the in vitro culture system of KRAS-mut colon cancer cells

Because it blocks VEGF-related angiogenesis, bevacizumab in combination with chemotherapy was approved by the US Food and Drug Administration (FDA) for the treatment of mCRC [42]. However, in our study, bevacizumab did not affect the viability of KRAS-mut colon cancer cells, even at a high concentration in an *in vitro* culture system (Supp. Fig. 1A). This result was consistent with that from a previous study in which bevacizumab blocked the binding of VEGF-A to endothelial cells via VEGF receptors (VEGFRs) during the process of pathological angiogenesis in the tumor microenvironment but did not directly inhibit the survival of tumor cells [43].

We next examined the effect of olaparib on the viability of KRAS-mut colon cancer cells. Under our experimental conditions, olaparib inhibited cell viability in a drug concentration–dependent manner (Supp. Fig. 1B). However, the presence of bevacizumab for 72 h did not influence sensitivity to olaparib in the cell lines HCT116, SW620, and Lovo (Supp. Fig. 1C).

Taken together, these findings suggested that olaparib had a dose-dependent effect on KRAS-mut colon cancer cells and that no additional inhibition could be obtained by combining it with bevacizumab *in vitro*. Therefore, combinational benefits should be further evaluated *in vivo*.

Bevacizumab + olaparib shrank KRAS-mut tumors in vivo

To verify whether olaparib affected the efficacy of bevacizumab against KRAS-mut colon cancer cells *in vivo*, we established subcutaneous-tumor models using HCT116 cells and the mice with olaparib, bevacizumab, or a combination thereof. As shown in Fig. 1A, continuous bevacizumab + olaparib treatment resulted in markedly greater tumor regression than treatment with either therapy alone. We observed no significant weight loss in any group of mice during the 20 days of treatment (Supp. Fig. 2). These data clearly indicated that bevacizumab improved the response of KRAS-mut tumors to olaparib treatment without significant toxicity.

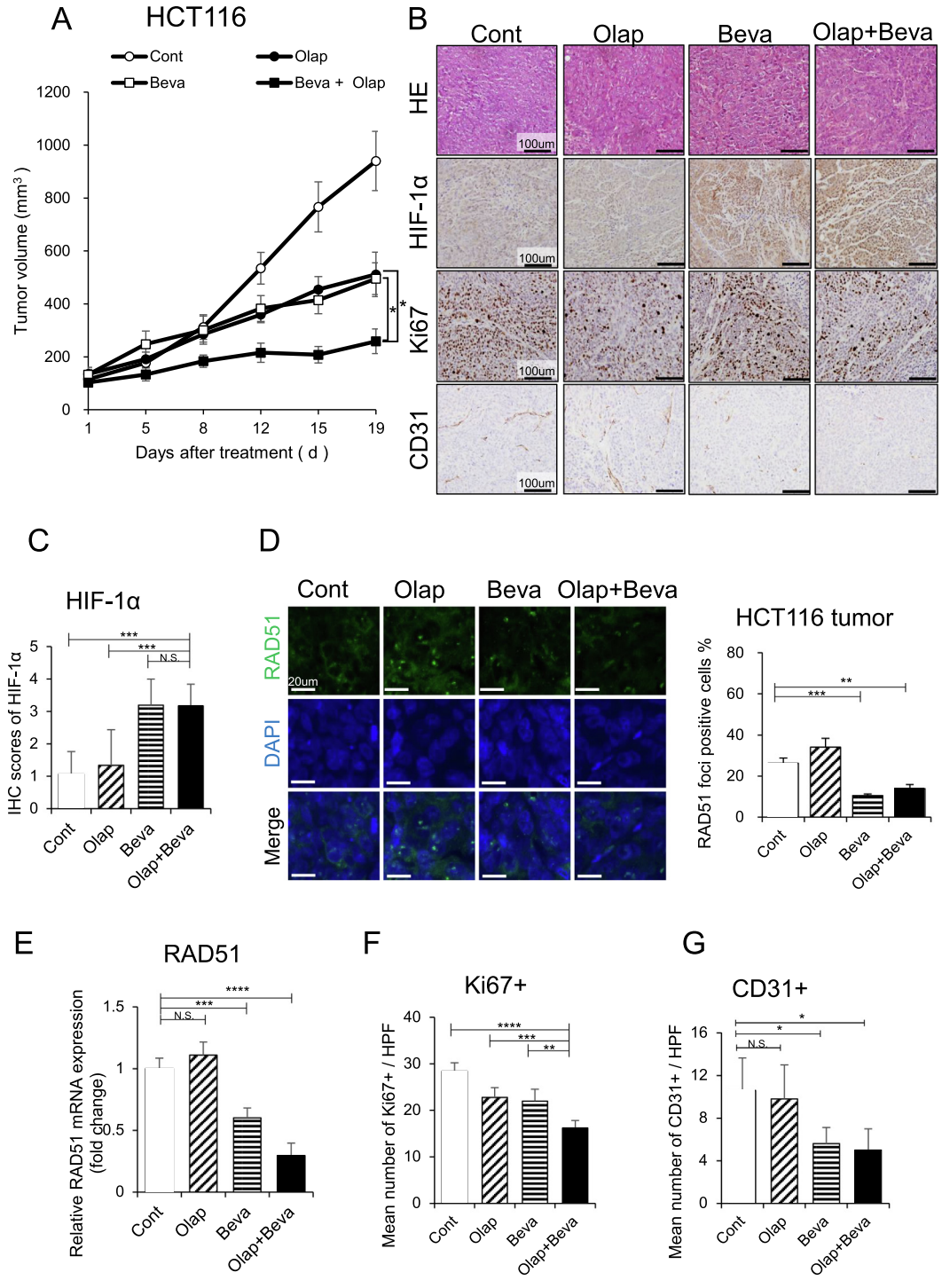

Fig. 1. Effects of bevacizumab and olaparib on human KRAS-mut CRC *in vivo*. (A) HCT116 cells (5×10^6 cells) were inoculated subcutaneously into nude mice, which then received oral olaparib (50 mg/kg/d; $n = 6$), intraperitoneal bevacizumab (5 mg/kg/twice weekly; $n = 6$), olaparib + bevacizumab ($n = 6$), or vehicle control ($n = 6$). Tumor size was measured twice weekly, and tumor volume was calculated as described in the ``Materials and Methods'' section. Error bars = SE. (B) Representative images of H&E staining and HIF-1α, Ki-67, and CD31 immunostaining of subcutaneous tumors established by injection of HCT116 cells (day 19). Scale bar = 100 μm. (C) Quantification of hypoxic cells in subcutaneous tumors, shown as IHC scores for HIF-1α. The data shown represent the mean þ SD of 5 areas. (D) Left: representative images of immunofluorescence staining showing the RAD51 foci in subcutaneous tumors. RAD51 and nuclei are shown in green (Alexa Fluor 488) and blue (DAPI), respectively, in the merged images. Scale bar = 20 μm. Right: quantification of the RAD51 foci formation. Data shown represent the mean þ SD of 3 areas. (E) qRT-PCR analysis of *RAD51* expression levels in the isolated tumor tissues; $n = 3$. Relative mRNA expression was normalized to GAPDH. (F) Quantification of proliferating cells in subcutaneous tumors, shown as the percentage of Ki-67-positive cells. (G) Quantification of tumor-associated endothelial cells in subcutaneous tumors, shown as the number of CD31-positive vessel fields. Data shown represent the mean þ SD of 5 areas. N.S. = non-significant. $^*P < 0.05$, $^{**}P < 0.01$, $^{***}P < 0.001$, and $^{****}P < 0.0001$ for the indicated comparisons by 1-way ANOVA. Cont = Control; Olap = Olaparib; Beva = Bevacizumab.

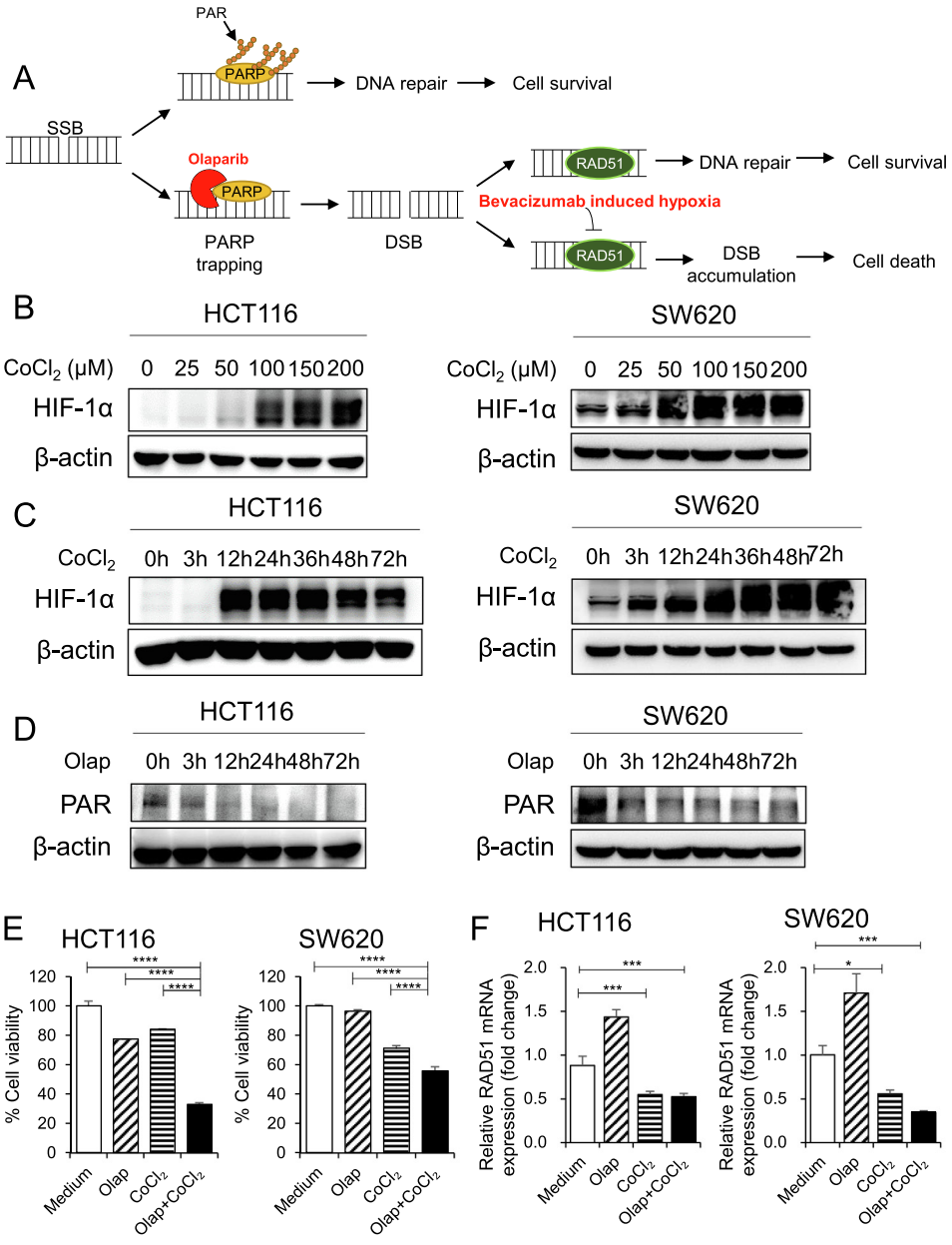

Fig. 2. $CoCl_2$-induced hypoxia in KRAS-mut colon cancer cells and sensitized cells to olaparib. (A) Working model for the effects of bevacizumab + olaparib combination therapy in replicating cells. Normally, SSBs activate PARP, and resulting SSB repair occurs through PAR of histones and recruitment of additional PARP-dependent repair proteins; DNA is repaired, and cells survive. Olaparib, a PARP inhibitor, inactivated the PARP-dependent repair system and consequently trapped PARP on DNA repair intermediates, obstructing replication forks, which created DSBs during DNA replication. DSBs can be repaired through HR, resulting in cell survival. Bevacizumab-induced hypoxia led to downregulation of HRR gene *RAD51*, impairing HRR; DSBs accumulated, causing cell death. To detect HIF-1α, we treated HCT116 and SW620 cells with $CoCl_2$ at the indicated (B) concentrations and (C) time points. (D) To detect PAR, we treated HCT116 and SW620 cells with olaparib (30 μM) at the indicated time points. Cells were lysed, and the indicated proteins were detected by Western blot. (E) We treated HCT116 and SW620 cells with or without $CoCl_2$ (100 μM) and/or olaparib (30 μM) for 72 h. Cell growth was measured via MTT assay. (F) We treated HCT116 and SW620 cells with or without $CoCl_2$ (100 μM) and/or olaparib (30 μM) for 72 h to examine *RAD51* expression using qRT-PCR. Relative mRNA expression was normalized to GAPDH. Each experiment was performed at least 3 times independently. Bars indicate SD. N.S. = non-significant. $^*P < 0.05$, $^{***}P < 0.001$, and $^{****}P < 0.0001$ for the indicated comparisons by 1-way ANOVA. Olap = Olaparib.

Bevacizumab damaged HRR via hypoxia, which increased the efficacy of olaparib in a subcutaneous-tumor model of KRAS-mut colon cancer cells

To explore whether bevacizumab could induce hypoxia and damage to HR, we confirmed our hypothesis using *in vivo* tumors. Via IHC staining for HIF-1α, we observed an obvious hypoxic area in the subcutaneous tumors treated continuously with bevacizumab (Fig. 1B and C). We next examined HR ability after bevacizumab or combination therapy in tumors using RAD51 focus formation experiment, since RAD51 foci that are microscopically visible are believed to represent sites of recombinational DNA repair[44,45]. As shown in Fig. 1D, RAD51 focus positive cells

were decreased significantly under the hypoxia situation by bevacizumab treatment (Fig. 1D). Collectively, bevacizumab inhibited the experiment of *RAD51* mRNA in both groups, and the phenomena was relatively obvious with bevacizumab + olaparib treatment (Fig. 1E). These results suggested that bevacizumab induced hypoxia, thereby increasing HRR defection, which might have resulted in an elevated sensitivity to olaparib.

To examine the efficacy of bevacizumab + olaparib *in vivo*, we next assessed tumor cell proliferation and microvessel density via IHC staining of subcutaneous tumors after treatment. Compared with vehicle and treatment with either bevacizumab or olaparib alone, combination treatment reduced the number of Ki-67-positive proliferating tumor cells and CD31-positive endothelial cells in KRAS-mut subcutaneous tumors (Fig. 1B, F, and G). These results indicated that olaparib + bevacizumab increased sensitivity to olaparib in a KRAS-mut colon cancer mouse model, presumably via damage to HRR induced by bevacizumab-caused hypoxia.

Hypoxia increased damage to HRR and sensitized KRAS-mut colon cancer cells to olaparib

Noting the synergistic effect of olaparib + bevacizumab *in vivo*, we chose $CoCl_2$ to mimic a hypoxic environment *in vitro* to explore the role of bevacizumab-induced hypoxia on olaparib (Fig. 2A). We selected 100 μmol/L $CoCl_2$, a dose reported to be able to induce molecular responses similar to those found in low-oxygen conditions in mammalian systems [46], after confirming the expression of induced-hypoxia protein HIF-1α in cell lines HCT116, SW620, and Lovo (Fig. 2B, Supp. Fig. 3A). $CoCl_2$ remarkably induced HIF-1α overexpression and sustained hypoxic conditions for at least 72 h (Fig. 2C, Supp. Fig. 3B). Meanwhile, we evaluated the biological activity of olaparib. Western blot results showed that olaparib could quickly inhibit PAR activity and sustain this effect for at least 72 h (Fig. 2D, Supp. Fig. 3C).

We next sought to evaluate the correlation between hypoxia and susceptibility to olaparib in KRAS-mut colon cancer cell lines. Cell viability of the above mentioned 3 tested cell lines was significantly inhibited by $CoCl_2$ + olaparib treatment (Fig. 2E, Supp. Fig. 3D).

To confirm the role of hypoxia on HRR, we analyzed the *RAD51* expression and RAD51 focus formation in KRAS-mut CRC cells in *vitro* using KRAS-mut cancer cell lines. Results shown that $CoCl_2$-induced hypoxia decreased *RAD51* expression (Fig. 2F, Supp. Fig. 3E). Meanwhile, the percentage of the RAD51 focus positive cells after $CoCl_2$ treatment, was significantly lower compared with control group, indicating an impaired HRR by hypoxia (Fig. 3A and B).

Taken together, these results clearly indicated that sensitivity to olaparib could be increased by damaging HR via hypoxia, which reduced the viability of KRAS-mut colon cancer cells.

Olaparib induced cell cycle arrest, apoptosis and DNA damage of KRAS-mut colon cancer cells under hypoxia situation

To investigate the underlying mechanism by which hypoxia enhanced cancer cells' sensitivity to olaparib, we performed both cell cycle and cell apoptosis assays on KRAS-mut CRC cells exposed to $CoCl_2$ and/or olaparib. Compared with either $CoCl_2$ or olaparib treatment alone, treatment

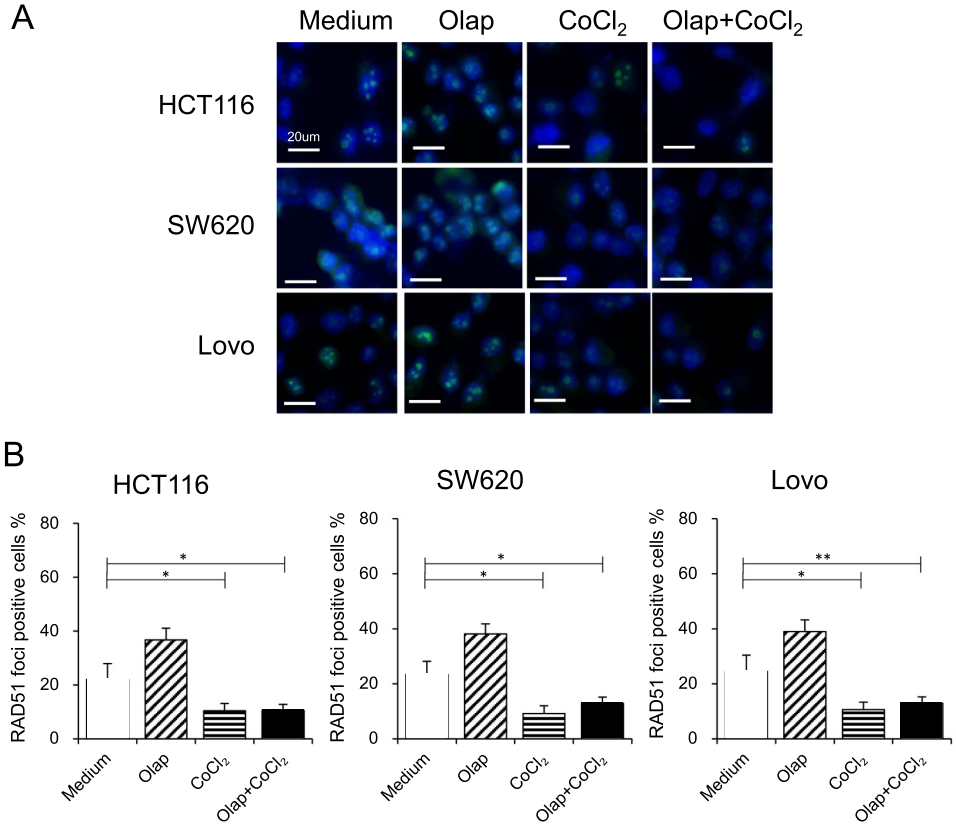

Fig. 3. $CoCl_2$ impaired HRR in KRAS-mut colon cancer cells. (A) Representative images of immunofluorescence staining showing the RAD51 foci in different groups for different cell lines. RAD51 and nuclei are shown in green (Alexa Fluor 488) and blue (DAPI), respectively, in the merged images. Scale bar = 20 μm. (B) Quantification of the RAD51 foci formation. Data shown represent the mean þ SD of 3 areas. $^*P < 0.05$ and $^{**}P < 0.01$ for the indicated comparisons by 1-way ANOVA. Olap = Olaparib.

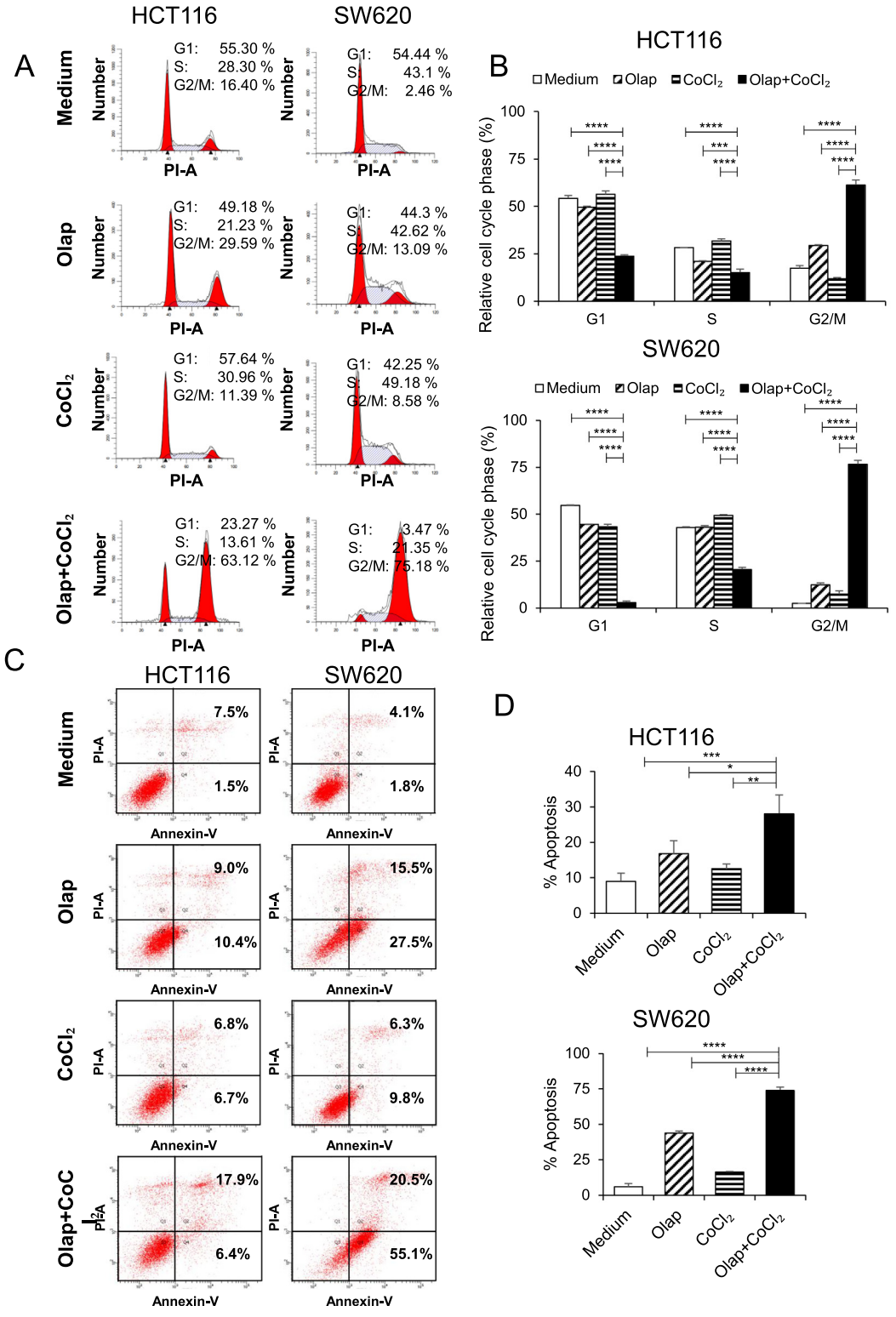

Fig. 4. Olaparib induced cell cycle arrest and apoptosis of KRAS-mut colon cancer cells under hypoxic conditions. (A) Flow cytometry (FCM) images with PI staining for analysis of cell cycle distribution in HCT116 and SW620 cells after treatment with or without $CoCl_2$ (100 μM) and/or olaparib (30 μM) for 72 h. (B) Proportions of HCT116 and SW620 cells in G1, S, and G2/M phases, presented as bar graphs. (C) We performed FCM analysis with Annexin V–PI staining to evaluate the percentage of HCT116 and SW620 cells that were apoptotic after treatment with or without $CoCl_2$ (100 μM) and/or olaparib (30 μM) for 72 h. (D) Total proportion of cells undergoing apoptosis, represented as bar graphs. Each experiment was performed at least 3 times independently. Bars indicate SD. N.S. = non-significant. $^{*}P < 0.05$, $^{**}P < 0.01$, $^{***}P < 0.001$, and $^{****}P < 0.0001$ for the indicated comparisons by 1-way ANOVA. Olap = Olaparib.

with $CoCl_2$ + olaparib treatment led to G2/M arrest (Fig. 4A and B, Supp. Fig. 3F and G). In addition, while treatment with either $CoCl_2$ or olaparib alone induced moderate apoptosis in HCT116 and SW620 cells, treatment with $CoCl_2$ + olaparib induced apoptosis to a striking degree (Fig. 4C and D). This indicated that hypoxia-mediated sensitivity to olaparib might be associated with increased cell apoptosis and cell cycle arrest.

An increased level of γ-H2AX is considered to be a marker of DNA damage [47]. Hence, we analyzed the γ-H2AX foci in cells under $CoCl_2$ treatment with or without olaparib. As shown in Fig. 5A and B, $CoCl_2$ treatment induced moderate DNA damage in cancer cells, while olaparib further enhanced the degree of DNA damage caused by $CoCl_2$ in KRAS-mut CRC cells.

Taken together, these results demonstrated that bevacizumab impaired HRR via hypoxia, providing additional benefit to olaparib in our subcutaneous-tumor model of KRAS-mut CRC. This antitumor effect might have been associated with cell cycle arrest, apoptosis and DNA damage.

Discussion

CRC is one of the major causes of cancer mortality worldwide [1]. Multiple monoclonal antibodies, such as cetuximab and bevacizumab—directed against human epidermal growth factor receptor 1 (HER1)/EGFR and VEGF, respectively—significantly improve the outcomes of patients with mCRC [23,48]. However, these drugs are less effective in the KRAS-mut subset of colon cancer [9,49–51]. Therefore, several clinical trials of combinational therapies have been conducted in this subset. In the present study, we confirmed the benefit of bevacizumab + olaparib in KRAS-mut colon cancer and further demonstrated that the underlying mechanism of this drug combination was impairment of HRR caused by bevacizumab-induced hypoxia.

Tumor hypoxia commonly occurs during the anti-angiogenic period and might play an important role in anti-angiogenic drug resistance [30–32]. Indeed, there is still some controversy over whether anti-angiogenic therapy, due to its heterogeneous effect, induces intratumor hypoxia in the tumor microenvironment. On the one hand, the traditional concept of anti-angiogenic therapy is to inhibit the formation of tumor blood vessels, thus aggravating tumor hypoxia. On the other hand, several studies have reported that anti-angiogenic therapy can normalize tumor vasculature, and thus improve tumor blood supply and ameliorate hypoxia [52–55]. In cancer cell-derived xenograft models of cervical cancer, malignant glioma, and CRC, increased hypoxic areas and elevated hypoxia markers were found after treatment with diverse doses of bevacizumab, including 10 mg/kg, 3 doses over 8 days [55]; 6 mg/kg, 3 times weekly [56]; and 0.5 or 5 mg/kg, twice weekly [57]. However, in other cancers, such as squamous-cell carcinoma of the head and neck, researchers using [(61)Cu]Cu-diacetyl-bis(N4-methylthiosemicarbazone) positron emission

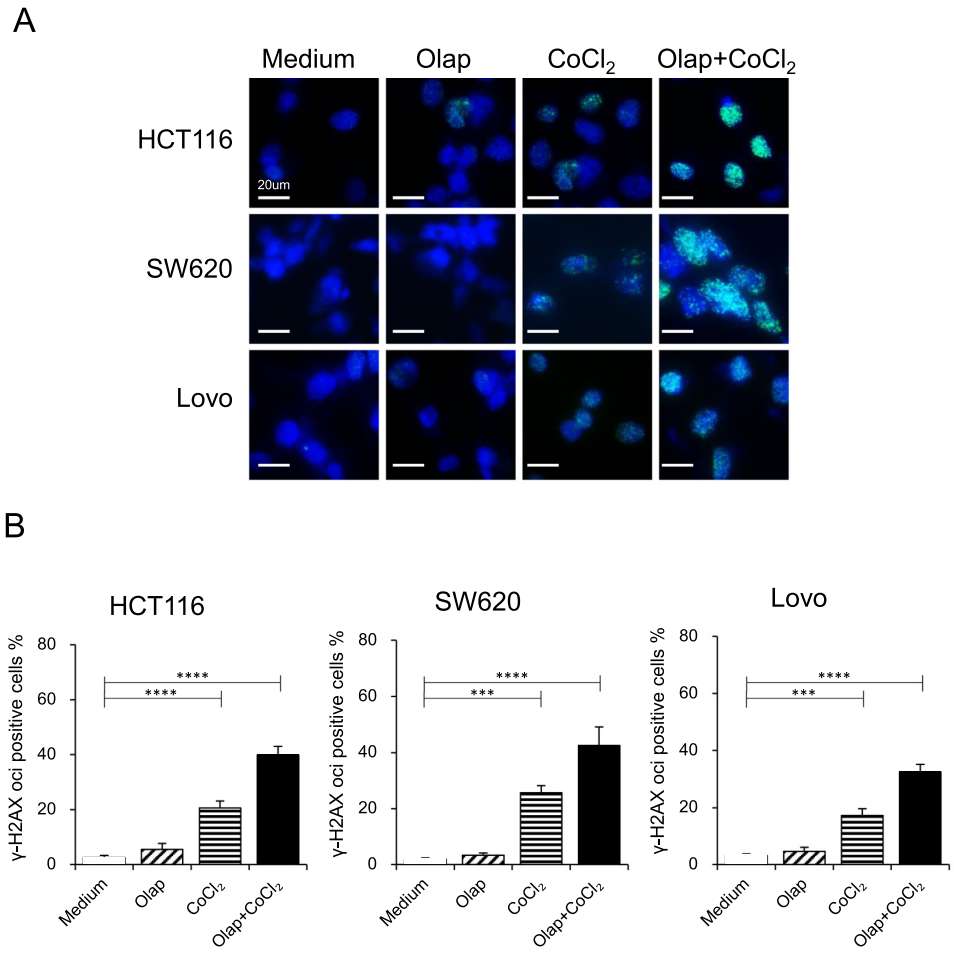

Fig. 5. Olaparib enhanced the degree of DNA damage caused by $CoCl_2$ in KRAS-mut colon cancer cells. (A) Representative images of immunofluorescence staining of γ-H2AX foci in different groups for different cell lines. γ-H2AX foci and nuclei are shown in green (Alexa Fluor 488) and blue (DAPI), respectively, in the merged images. Scale bar = 20 μm. (B) Quantification of the γH2AX foci formation. Data shown represent the mean þ SD of 3 areas. N.S. = non-significant. ***P < 0.001, and ****P < 0.0001 for the indicated comparisons by 1-way ANOVA. Cont = Control; Olap = Olaparib; Beva = Bevacizumab.

tomography (Cu-ATSM PET) detected significant reductions in tumor hypoxia after bevacizumab monotherapy [58]. In our setting, at a twice-weekly dose of 5 mg/kg bevacizumab, hypoxic areas and hypoxia markers of HIF-1α in the tumor microenvironment increased; this was accompanied by tumor vascular regression, which was marked by CD31-positive endothelial cells. Taken together, these findings showed that bevacizumab treatment increased oxygenation in some experimental tumors and induced hypoxia in others. This might have been due to differences in tumor type, duration of administration, and dose.

Olaparib was approved by the FDA in December 2014 for advanced ovarian-cancer patients with a deleterious germline mutation of *BRCA1* or *BRCA2* [59]. Similar to *BRCA1*, *RAD51* is another famous HRR gene that plays a central role in DSB repair [60,61]. In our study, bevacizumab-induced hypoxia reduced the expression of *RAD51* gene and the formation of RAD51 foci, suggesting damage to HRR; this observation was consistent with previous reports [34–36]. Disruption of such HR protein conferred sensitivity to PARP inhibitors and displayed marked antitumor effects in an HCT116 CRC xenograft model. Meanwhile, bevacizumab + olaparib was well tolerated in the mouse model, which was consistent with clinical practice for advanced solid tumors [37]. olaparib + cediranib, a VEGFR antagonist, is also reported to be tolerable and to improve PFS compared with olaparib alone in patients with recurrent platinum-sensitive high-grade serous or endometrioid ovarian cancer [62,63]. Additionally, in the phase 3 Platine, Avastin, and OLAparib in First-line Therapy (PAOLA-1) trial, the addition of maintenance therapy to olaparib led to a statistically significant improvement in PFS in patients with advanced ovarian cancer receiving first-line standard therapy including bevacizumab, with a substantial benefit in patients with homologous recombination deficiency (HRD)-positive tumors [38].

Encouraged by the above-mentioned good tolerance and outcomes, in our present study, we sought further insight into the potential mechanism of bevacizumab + olaparib. We used $CoCl_2$ to mimic hypoxia [64,65] *in vitro* and to clarify the potential role of combined therapy. $CoCl_2$ induced hypoxic response, which was confirmed by elevated HIF-1α protein expression in $CoCl_2$-treated cells in a time- and concentration-dependent manner. In addition, consistent with our *in vivo* findings, we found that $CoCl_2$ markedly downregulated expression levels of *RAD51* mRNA and the percentage of the RAD51 focus positive cells, indicating an impaired HRR by hypoxia. Moreover, we confirmed that $CoCl_2$-induced hypoxia could sensitize KRAS-mut CRC cells to olaparib by inducing additional DNA damage, cell apoptosis and cell cycle arrest in the G2/M phase. Our present data demonstrated the promising efficacy of olaparib + bevacizumab against KRAS-mut CRC. It will be interesting to evaluate this combination in other KRAS-mut tumor types, such as lung and pancreatic cancers. It will also be necessary to further clarify the potential relationship between KRAS mutations and HR, as well as the underlying mechanism of bevacizumab-induced hypoxia.

Conclusion

In conclusion, our findings suggested that bevacizumab led to hypoxia in the tumor microenvironment and induced HR deficiency in KRAS-mut cells. Therefore, it increased the effectiveness of olaparib, which might have occurred via G2/M phase arrest and DNA damage. These findings provide a rationale for this combination treatment in KRAS-mut CRC patients.

Declaration of Competing Interest

The authors declare that they have no known competing financial interests or personal relationships that could have appeared to influence the work reported in this paper.

Acknowledgements

We would like to express our sincere thanks to Department of Radiation Oncology, Nanfang Hospital and Southern Medical University. We thank LetPub (www.letpub.com) for its linguistic assistance during the preparation of this manuscript.

Funding

This work was supported by the National Natural Science Foundation of China (Grant No. 81572966); the Natural Science Foundation of Guangdong Province (Grant No. 2017A030313883); and Postdoctoral Science Foundation of China (Grant No. 2019M663002).

Appendix A. Supplementary data

Supplementary data to this article can be found online at https://doi.org/10.1016/j.neo.2020.06.001.

References

1. Bray F, Ferlay J, Soerjomataram I, Siegel RL, Torre LA, Jemal A. Global cancer statistics 2018: GLOBOCAN estimates of incidence and mortality worldwide for 36 cancers in 185 countries. *CA Cancer J Clin* 2018;**68**:394–424.
2. Tjandra JJ, Chan MK. Follow-up after curative resection of colorectal cancer: a meta-analysis. *Dis Colon Rectum* 2007;**50**:1783–99.
3. Peeters M, Kafatos G, Taylor A, Gastanaga VM, Oliner KS, Hechmati G, Terwey JH, van Krieken JH. Prevalence of RAS mutations and individual variation patterns among patients with metastatic colorectal cancer: A pooled analysis of randomised controlled trials. *Eur J Cancer (Oxford, England: 1990)* 2015;**51**:1704–13.
4. Modest DP, Ricard I, Heinemann V, Hegewisch-Becker S, Schmiegel W, Porschen R, Stintzing S, Graeven U, Arnold D, von Weikersthal LF, et al. Outcome according to KRAS-, NRAS- and BRAF-mutation as well as KRAS mutation variants: pooled analysis of five randomized trials in metastatic colorectal cancer by the AIO colorectal cancer study group. *Ann Oncol* 2016;**27**:1746–53.
5. Douillard JY, Oliner KS, Siena S, Tabernero J, Burkes R, Barugel M, Humblet G, Bodoky G, Cunningham D, Jassem J, et al. Panitumumab-FOLFOX4 treatment and RAS mutations in colorectal cancer. *N Engl J Med* 2013;**369**:1023–34.
6. Van Cutsem E, Kohne CH, Hitre E, Zaluski J, Chang Chien CR, Makhson A, D'Haens G, Pinter T, Lim R, Bodoky G, et al. Cetuximab and chemotherapy as initial treatment for metastatic colorectal cancer. *N Engl J Med* 2009;**360**:1408–17.
7. Karapetis CS, Khambata-Ford S, Jonker DJ, O'Callaghan CJ, Tu D, Tebbutt RJ, Simes RJ, Chalchal H, Shapiro JD, Robitaille S, et al. K-ras mutations and benefit from cetuximab in advanced colorectal cancer. *N Engl J Med* 2008;**359**:1757–65.
8. Van Cutsem E, Lenz HJ, Kohne CH, Heinemann V, Tejpar S, Melezinek I, Beier F, Stroh C, Rougier P, van Krieken JH, et al. Fluorouracil, leucovorin, and irinotecan plus cetuximab treatment and RAS mutations in colorectal cancer. *J Clin Oncol* 2015;**33**:692–700.
9. Tol J, Koopman M, Cats A, Rodenburg CJ, Creemers GJ, Schrama JG, Erdkamp FL, Vos AH, van Groeningen CJ, Sinnige HA, et al. Chemotherapy, bevacizumab, and cetuximab in metastatic colorectal cancer. *N Engl J Med* 2009;**360**:563–72.
10. Andreyev HJ, Norman AR, Cunningham D, Oates J, Dix BR, Iacopetta BJ, Young J, Walsh T, Ward R, Hawkins N, et al. Kirsten ras mutations in patients with colorectal cancer: the 'RASCAL II' study. *Br J Cancer* 2001;**85**:692–6.
11. Andreyev HJ, Norman AR, Cunningham D, Oates JR, Clarke PA. Kirsten ras mutations in patients with colorectal cancer: the multicenter ``RASCAL'' study. *J Natl Cancer Inst* 1998;**90**:675–84.
12. Cox AD, Fesik SW, Kimmelman AC, Luo J, Der CJ. Drugging the undruggable RAS: Mission possible? *Nat Rev Drug Discovery* 2014;**13**:828–51.

13. Bos JL, Rehmann H, Wittinghofer A. GEFs and GAPs: critical elements in the control of small G proteins. *Cell* 2007;**129**:865–77.
14. Feuerstein J, Kalbitzer HR, John J, Goody RS, Wittinghofer A (1987). Characterisation of the metal-ion-GDP complex at the active sites of transforming and nontransforming p21 proteins by observation of the 17O-Mn superhyperfine coupling and by kinetic methods, Eur J Biochem, 162, 49–55.
15. Sun Q, Burke JP, Phan J, Burns MC, Olejniczak ET, Waterson AG, Lee OW, Rossanese OW, Fesik SW. Discovery of small molecules that bind to K-Ras and inhibit Sos-mediated activation. *Angew Chem (Engl)* 2012;**51**:6140–3.
16. Gilmartin AG, Bleam MR, Groy A, Moss KG, Minthorn EA, Kulkarni SG, Rominger CM, Erskine S, Fisher KE, Yang J, et al. GSK1120212 (JTP-74057) is an inhibitor of MEK activity and activation with favorable pharmacokinetic properties for sustained in vivo pathway inhibition. *Clin Cancer Res* 2011;**17**:989–1000.
17. Engelman JA, Chen L, Tan X, Crosby K, Guimaraes AR, Upadhyay R, Maira K, McNamara K, Perera SA, Song Y, et al. Effective use of PI3K and MEK inhibitors to treat mutant Kras G12D and PIK3CA H1047R murine lung cancers. *Nat Med* 2008;**14**:1351–6.
18. Hatzivassiliou G, Song K, Yen I, Brandhuber BJ, Anderson DJ, Alvarado R, Ludlam MJ, Stokoe D, Gloor SL, Vigers G, et al. RAF inhibitors prime wild-type RAF to activate the MAPK pathway and enhance growth. *Nature* 2010;**464**:431–5.
19. Heidorn SJ, Milagre C, Whittaker S, Nourry A, Niculescu-Duvas I, Dhomen J, Hussain J, Reis-Filho JS, Springer CJ, Pritchard C, et al. Kinase-dead BRAF and oncogenic RAS cooperate to drive tumor progression through CRAF. *Cell* 2010;**140**:209–21.
20. Bennouna J, Lang I, Valladares-Ayerbes M, Boer K, Adenis A, Escudero P, Kim TY, Pover GM, Morris CD, Douillard JY. A Phase II, open-label, randomised study to assess the efficacy and safety of the MEK1/2 inhibitor AZD6244 (ARRY-142886) versus capecitabine monotherapy in patients with colorectal cancer who have failed one or two prior chemotherapeutic regimens. *Invest New Drugs* 2011;**29**:1021–8.
21. Macarulla T, Tabernero J, Cervantes A, Rosello S, Van Cutsem E, Tejpar S, Prenen H, Martinelli E, Troiani T, Campana F, et al. Phase I/Ii study of Folfiri plus the Mek1/2 inhibitor pimasertib (Msc1936369b) as second-line treatment for Kras mutated metastatic colorectal cancer. *Ann Oncol* 2012;**23**:27.
22. Genentech Inc. Avastin® (bevacizumab) prescribing information. 2004 (last update 2019). https://www.accessdata.fda.gov/drugsatfda_docs/label/2019/125085s331lbl.pdf.
23. Hurwitz H, Fehrenbacher L, Novotny W, Cartwright T, Hainsworth J, Heim J, Berlin J, Baron A, Griffing S, Holmgren E, et al. Bevacizumab plus irinotecan, fluorouracil, and leucovorin for metastatic colorectal cancer. *N Engl J Med* 2004;**350**:2335–42.
24. Giantonio BJ, Catalano PJ, Meropol NJ, O'Dwyer PJ, Mitchell EP, Alberts SR, Schwartz MA, Benson AB, 3rd (2007). Bevacizumab in combination with oxaliplatin, fluorouracil, and leucovorin (FOLFOX4) for previously treated metastatic colorectal cancer: results from the Eastern Cooperative Oncology Group Study E3200, J Clin Oncol, 25, 1539–1544.
25. Bennouna J, Sastre J, Arnold D, Osterlund P, Greil R, Van Cutsem E, von Moos R, Vieitez JM, Bouche O, Borg C, et al. Continuation of bevacizumab after first progression in metastatic colorectal cancer (ML18147): a randomised phase 3 trial. *Lancet Oncol* 2013;**14**:29–37.
26. Kabbinavar FF, Schulz J, McCleod M, Patel T, Hamm JT, Hecht JR, Mass R, Perrou B, Nelson B, Novotny WF. Addition of bevacizumab to bolus fluorouracil and leucovorin in first-line metastatic colorectal cancer: results of a randomized phase II trial. *J Clin Oncol* 2005;**23**:3697–705.
27. Wang S, Xiao Z, Hong Z, Jiao H, Zhu S, Zhao Y, Bi J, Qiu J, Zhang D, Yan J, et al. FOXF1 promotes angiogenesis and accelerates bevacizumab resistance in colorectal cancer by transcriptionally activating VEGFA. *Cancer Lett* 2018;**439**:78–90.
28. Jahangiri A, Nguyen A, Chandra A (2017). Cross-activating c-Met/beta1 integrin complex drives metastasis and invasive resistance in cancer, 114, E8685–E8694.
29. Schiffmann LM, Fritsch M, Gebauer F, Gunther SD, Stair NR, Seeger JM, Thangarajah F, Dieplinger G, Bludau M, Alakus H, et al. Tumour-infiltrating neutrophils counteract anti-VEGF therapy in metastatic colorectal cancer. *Br J Cancer* 2019;**120**:69–78.
30. Pennacchietti S, Michieli P, Galluzzo M, Mazzone M, Giordano S, Comoglio PM. Hypoxia promotes invasive growth by transcriptional activation of the met protooncogene. *Cancer Cell* 2003;**3**:347–61.
31. Carbonell WS, DeLay M, Jahangiri A, Park CC, Aghi MK. beta1 integrin targeting potentiates antiangiogenic therapy and inhibits the growth of bevacizumab-resistant glioblastoma. *Cancer Res* 2013;**73**:3145–54.
32. Sidorov M, Jahangiri A, Han S-W, De Lay M, Wagner J, Castro B, Flanigan PM, Imber BS, Weiss WA, Aghi MK (2016). 340c-Met/beta1 integrin: a receptor complex driving invasive glioblastoma resistance to antiangiogenic therapy, Neurosurgery 63(Suppl 1), 199–200.
33. Hu YL, DeLay M, Jahangiri A, Molinaro AM, Rose SD, Carbonell WS, Aghi MK. Hypoxia-induced autophagy promotes tumor cell survival and adaptation to antiangiogenic treatment in glioblastoma. *Cancer Res* 2012;**72**:1773–83.
34. Bindra RS, Gibson SL, Meng A, Westermark U, Jasin M, Pierce AJ, Bristow MK, Classon MK, Glazer PM. Hypoxia-induced down-regulation of BRCA1 expression by E2Fs. *Cancer Res* 2005;**65**:11597–604.
35. Bindra RS, Schaffer PJ, Meng A, Woo J, Maseide K, Roth ME, Lizardi P, Hedley DW, Bristow RG, Glazer PM. Down-regulation of Rad51 and decreased homologous recombination in hypoxic cancer cells. *Mol Cell Biol* 2004;**24**:8504–18.
36. Hegan DC, Lu Y, Stachelek GC, Crosby ME, Bindra RS, Glazer PM (2010). Inhibition of poly(ADP-ribose) polymerase down-regulates BRCA1 and RAD51 in a pathway mediated by E2F4 and p130, Proc Natl Acad Sci USA, 107, 2201–2206.
37. Dean E, Middleton MR, Pwint T, Swaisland H, Carmichael J, Goodege-Kunwar P, Ranson M. Phase I study to assess the safety and tolerability of olaparib in combination with bevacizumab in patients with advanced solid tumours. *Br J Cancer* 2012;**106**:468–74.
38. Ray-Coquard I, Pautier P, Pignata S, Perol D, Gonzalez-Martin A, Berger R, Fujiwara K, Vergote I, Colombo N, Maenpaa J, et al. Olaparib plus Bevacizumab as First-Line Maintenance in Ovarian Cancer. *N Engl J Med* 2019;**381**:2416–28.
39. LYNPARZA® (olaparib) tablets, for oral use Initial U.S. Approval: 2014 (last update 2018). https://www.accessdata.fda.gov/drugsatfda_docs/label/2018/208558s006lbl.pdf.
40. de Murcia JM, Niedergang C, Trucco C, Ricoul M, Dutrillaux B, Mark M, Oliver FJ, Masson M, Dierich A, LeMeur M, et al. (1997). Requirement of poly(ADP-ribose) polymerase in recovery from DNA damage in mice and in cells, Proc Natl Acad Sci USA, 94, 7303–7307.
41. Yano S, Wang W, Li Q, Matsumoto K, Sakurama H, Nakamura T, Ogino H, Kakiuchi S, Hanibuchi M, Nishioka Y, et al. Hepatocyte growth factor induces gefitinib resistance of lung adenocarcinoma with epidermal growth factor receptor-activating mutations. *Cancer Res* 2008;**68**:9479–87.
42. Rosen LS, Jacobs IA, Burkes RL. Bevacizumab in colorectal cancer: current role in treatment and the potential of biosimilars. *Target Oncol* 2017;**12**:599–610.
43. Ferrara N, Hillan KJ, Gerber HP. Discovery and development of bevacizumab, an anti-VEGF antibody for treating cancer. *Nat Rev Drug Discovery* 2004;**3**:391–400.
44. Liu Y, Maizels N. Coordinated response of mammalian Rad51 and Rad52 to DNA damage. *EMBO Rep* 2000;**1**:85–90.
45. Tashiro S, Walter J, Shinohara A, Kamada N, Cremer T. Rad51 accumulation at sites of DNA damage and in postreplicative chromatin. *J Cell Biol* 2000;**150**:283–91.
46. Yang SJ, Pyen J, Lee I, Lee H, Kim Y, Kim T. Cobalt chloride-induced apoptosis and extracellular signal-regulated protein kinase 1/2 activation in rat C6 glioma cells. *J Biochem Mol Biol* 2004;**37**:480–6.
47. Podhorecka M, Skladanowski A, Bozko P (2010). H2AX phosphorylation: its role in DNA damage response and cancer therapy, J Nucleic Acids 2010.
48. Cremolini C, Loupakis F, Antoniotti C, Lupi C, Sensi E, Lonardi S, Mezi S, Tomasello G, Ronzoni M, Zaniboni A, et al. FOLFOXIRI plus bevacizumab versus FOLFIRI plus bevacizumab as first-line treatment of patients with metastatic colorectal cancer: updated overall survival and molecular subgroup analyses of the open-label, phase 3 TRIBE study. *Lancet Oncol* 2015;**16**:1306–15.
49. Van Cutsem E, Kohne CH, Lang I, Folprecht G, Nowacki MP, Cascinu S, Shchepotin I, Maurel J, Cunningham D, Tejpar S, et al. Cetuximab plus irinotecan, fluorouracil, and leucovorin as first-line treatment for metastatic colorectal cancer: updated analysis of overall survival according to tumor KRAS and BRAF mutation status. *J Clin Oncol* 2011;**29**:2011–9.

50. Schwartzberg LS, Rivera F, Karthaus M, Fasola G, Canon JL, Hecht JR, Yu H, Oliner KS, Go WY. PEAK: a randomized, multicenter phase II study of panitumumab plus modified fluorouracil, leucovorin, and oxaliplatin (mFOLFOX6) or bevacizumab plus mFOLFOX6 in patients with previously untreated, unresectable, wild-type KRAS exon 2 metastatic colorectal cancer. *J Clin Oncol* 2014;**32**:2240–7.
51. Amado RG, Wolf M, Peeters M, Van Cutsem E, Siena S, Freeman DJ, Juan T, Sikorski R, Suggs S, Radinsky R, et al. (2008). Wild-type KRAS is required for panitumumab efficacy in patients with metastatic colorectal cancer, J Clin Oncol, 26, 1626–1634.
52. De Bock K, Mazzone M, Carmeliet P. Antiangiogenic therapy, hypoxia, and metastasis: risky liaisons, or not? *NatureReviews Clinical oncology* 2011;**8**:393–404.
53. Jain RK (2005). Normalization of tumor vasculature: an emerging concept in antiangiogenic therapy, Science (New York, NY) 307, 58–62.
54. Cantelmo AR, Pircher A, Kalucka J, Carmeliet P. Vessel pruning or healing: endothelial metabolism as a novel target? *Expert Opin Ther Targets* 2017;**21**:239–47.
55. Hauge A, Gaustad JV, Huang R, Simonsen TG, Wegner CS, Andersen LMK, Rofstad EK. DCE-MRI and quantitative histology reveal enhanced vessel maturation but impaired perfusion and increased hypoxia in bevacizumab-treated cervical carcinoma. *Int J Radiat Oncol Biol Phys* 2019;**104**:666–76.
56. Mori H, Yao Y, Learman BS, Kurozumi K, Ishida J, Ramakrishnan SK, Overmyer KA, Xue X, Cawthorn WP, Reid MA, et al. Induction of WNT11 by hypoxia and hypoxia-inducible factor-1alpha regulates cell proliferation, migration and invasion. *Sci Rep* 2016;**6**:21520.
57. Schiffmann LM, Brunold M, Liwschitz M, Goede V, Loges S, Wroblewski M, Quaas A, Alakus H, Stippel D, Bruns CJ, et al. A combination of low-dose bevacizumab and imatinib enhances vascular normalisation without inducing extracellular matrix deposition. *Br J Cancer* 2017;**116**:600–8.
58. Nyflot MJ, Kruser TJ, Traynor AM, Khuntia D, Yang DT, Hartig GK, McCulloch TM, Wiederholt PA, Gentry LR, Hoang T, et al. Phase 1 trial of bevacizumab with concurrent chemoradiation therapy for squamous cell carcinoma of the head and neck with exploratory functional imaging of tumor hypoxia, proliferation, and perfusion. *Int J Radiat Oncol Biol Phys* 2015;**91**:942–51.
59. Munroe M, Kolesar J. Olaparib for the treatment of BRCA-mutated advanced ovarian cancer. *Am J Health-system Pharm* 2016;**73**:1037–41.
60. Baumann P, West SC. Role of the human RAD51 protein in homologous recombination and double-stranded-break repair. *Trends Biochem Sci* 1998;**23**:247–51.
61. Krejci L, Altmannova V, Spirek M, Zhao X. Homologous recombination and its regulation. *Nucleic Acids Res* 2012;**40**:5795–818.
62. Liu JF, Tolaney SM, Birrer M, Fleming GF, Buss MK, Dahlberg SE, Lee H, Whalen C, Tyburski K, Winer E, et al. A Phase 1 trial of the poly(ADP-ribose) polymerase inhibitor olaparib (AZD2281) in combination with the anti-angiogenic cediranib (AZD2171) in recurrent epithelial ovarian or triple-negative breast cancer. *Eur J Cancer (Oxford, England: 1990)* 2013;**49**:2972–8
63. Liu JF, Barry WT, Birrer M, Lee JM, Buckanovich RJ, Fleming GF, Rimel B, Buss MK, Nattam S, Hurteau J, et al. Combination cediranib and olaparib versus olaparib alone for women with recurrent platinum-sensitive ovarian cancer: a randomised phase 2 study. *Lancet Oncol* 2014;**15**:1207–14.
64. Piret JP, Mottet D, Raes M, Michiels C (2002). CoCl2, a chemical inducer of hypoxia-inducible factor-1, and hypoxia reduce apoptotic cell death in hepatoma cell line HepG2, Ann N Y Acad Sci, 973, 443-447.
65. Park H, Lee DS, Yim MJ, Choi YH, Park S, Seo SK, Choi JS, Jang WH, Yea WS, Park WS, et al. 3,3′-Diindolylmethane inhibits VEGF expression through the HIF-1alpha and NF-kappaB pathways in human retinal pigment epithelial cells under chemical hypoxic conditions. *Int J Mol Med* 2015;**36**:301–8.